Cell Death and Differentiation (2004) 11, 1133–1145

www.nature.com/cdd

Cardiolipin and its metabolites move from mitochondria to other cellular membranes during death receptor-mediated apoptosis

M Sorice*,[1], A Circella[1], IM Cristea[2], T Garofalo[1], L Di Renzo[1], C Alessandri[3], G Valesini[3] and M Degli Esposti[4]

[1] Dipartimento di Medicina Sperimentale e Patologia, Università 'La Sapienza', Roma, Italy
[2] Michael Barber Centre for Mass Spectrometry, UMIST, Manchester, UK
[3] Dipartimento di Clinica e Terapia Medica Applicata, Cattedra di Reumatologia, Università 'La Sapienza', Roma, Italy
[4] School of Biological Sciences, The University of Manchester, UK
* Corresponding author: M Sorice. Tel: +39 06 49972675; Fax: +39 06 4454820; E-mail: maurizio.sorice@uniroma1.it

Received 10.11.03; revised 04.2.04; accepted 23.3.04; published online 04.6.04
Edited by D Vaux

Abstract

We previously reported that during death receptor-mediated apoptosis, cardiolipin (CL) relocates to the cell surface, where it reacts with autoantibodies from antiphospholipid syndrome sera. Here, we analysed the intracellular distribution of CL and its metabolites during the early phase of cell death signalling triggered by Fas stimulation in U937 cells and mouse liver. We found a redistribution of mitochondrial CL to the cell surface by using confocal microscopy and flow cytometry. Mass spectrometry revealed that CL and its metabolites relocated from mitochondria to other intracellular organelles during apoptosis, with a conversion into non-mitochondrial lipids. Concomitantly, cytosolic Bid relocated to the light membranes comprised in fraction P100, including the plasma membrane and associated vesicular systems. A direct Bid–CL interaction was demonstrated by the observation that CL and monolysoCL coimmunoprecipitated with Bid especially after Fas stimulation, suggesting a dynamic interaction of the protein with CL and its metabolites.

Cell Death and Differentiation (2004) **11,** 1133–1145.
doi:10.1038/sj.cdd.4401457
Published online 4 June 2004

Keywords: cardiolipin; phospholipids; mitochondria; Bid

Abbreviations: APG, acyl-phosphatidylglycerol; APS, antiphospholipid syndrome; CL, cardiolipin; DAG, diacyl-glycerol; DCL, di-lysocardiolipin; ER, endoplasmic reticulum; LBPA, lyso-bis-phosphatidic acid; MCL, mono-lysocardiolipin; MS, mass spectrometry; NDGA, nordihydroguaiaretic acid; PC, phosphatidylcholine; PC-PLC, phosphatidylcholine-specific phospholipase C; PE, phosphatidylethanolamine; PG, phosphatidylglycerol; PGP, phosphatidylglycerol-phosphate; PI, phosphatidylinositol; PIP, phosphatidylinositol-phosphate; PLA-2, phospholipase A2; PS, phosphatidylserine; SLBPA, semi-lyso-bis-phosphatidic acid; SM, sphingomyelin; TMRE, tetramethyl-rhodamine-ethyl-ester; z-VAD-FMK, z-Val-Ala-Asp-fluoromethyl ketone

Introduction

Apoptosis or cell death represents a key process in the homeostasis of the immune system[1,2] that is accompanied by characteristic ultrastructural modifications, including cell shrinkage, membrane blebbing, nuclear chromatin condensation and DNA laddering.[1–4] In addition, apoptosis has been reported to induce changes in the remodelling of membrane lipids.[5–8] Physiologically, phosphatidylcholine (PC) and sphingomyelin (SM) are almost exclusively located in the outer leaflet of the plasma membrane, while phosphatidylserine (PS) and 70% of phosphatidylethanolamine (PE) are located in the inner leaflet of the plasma membrane.[9] Apoptosis-induced changes in the intracellular location of phospholipids are well documented for PS, which is translocated to the outer leaflet of the plasma membrane as a consequence of downregulation of the ATP-dependent aminophospholipid translocase and an activation of a nonspecific lipid scramblase.[5–7]

The negatively charged lipid cardiolipin (CL), which is normally confined to the mitochondrial inner membrane,[10] has also been shown to undergo alterations in its traffic and remodelling during apoptosis.[8,11,12] In particular, it has been reported that CL moves to the outer leaflet of inner mitochondrial membrane in apoptotic cells[11] and, in another cell system, becomes exposed onto the cell surface.[12] Changes in CL distribution appeared to occur prior or concomitantly to membrane exposure of PS, but after the onset of an overproduction of reactive oxygen species (ROS).[11] The importance of lipid traffic in apoptosis is highlighted by the observation that Bid, a proapoptotic protein of the Bcl-2 family that is involved in death receptor-mediated death in many cell types,[13–16] displays lipid transfer activity between endoplasmic reticulum (ER) and mitochondria.[17] The preferential interaction with negatively charged phospholipids such as phosphatidylglycerol (PG) and its derivative CL[17,18] has suggested that Bid may be involved in the metabolic cycle of CL.[8]

We have evaluated this possibility in light of our previous observation that CL becomes exposed on the surface of cells undergoing apoptosis,[12] which has been documented also using α-CL antibodies selected from patients with the antiphospholipid antibody syndrome (APS).[19] In particular, we studied how Bid, which is required for mediating mitochondrial membrane damage during Fas-induced apoptosis,[15,16] might be involved in the intracellular transport of CL (as well as its metabolites) and potentially account for its relocation onto the plasma membrane of Fas-stimulated cells. We thus undertook a detailed study of the cellular events occurring early after Fas stimulation of a sensitive cell line (U937), with specific attention to the intracellular redistribution of Bid and mitochondrial lipids. We report here novel data demonstrating that CL and its metabolites relocate from mitochondria to other

intracellular organelles, and that during apoptosis CL is degraded and converted into non-mitochondrial lipids.

Results

CL relocates to the plasma membrane of U937 cells during Fas-mediated apoptosis

Apoptosis induces significant changes in the lipid composition of mitochondrial membranes,[8,11,20–23] which invariably include a decrease in CL – see McMillin and Dowhan[23] for a review. One possibility to explain the early decrease in mitochondrial CL is enhanced remodelling with increased traffic to other intracellular organelles, where degradation or recycling may occur.[8,23] In line with this possibility, we previously observed that cells undergoing death receptor-mediated apoptosis presented with CL on their plasma membrane.[12] As this observation implied relocation of CL outside mitochondria, presumably via other intracellular membranes like endosomes, we studied in more detail the immunoreactive presence of CL in cells undergoing Fas-mediated apoptosis.

We analysed first the distribution of CL in U937 cells by scanning confocal microscopy after double staining with a specific anti-CL antibody[12] and Mito Tracker Green FM as a mitochondrial marker (Figure 1). As expected, untreated U937 cells showed anti-CL staining confined to the cytoplasm, with pronounced granularity and without significant staining of the cell surface (Figure 1a, panel 1). Induction of apoptosis by treatment with an anti-Fas agonist for 1 h changed the cellular distribution of anti-CL reactivity, with an uneven surface distribution of the staining that appeared to cluster around plasma membrane (Figure 1a, panel 2). In untreated cells, the merged image of anti-CL staining and mitochondria labelled with Mito Tracker Green FM showed a pronounced colocalization, as revealed by brown–yellow areas, resulting from the overlap of green and red fluorescence (Figure 1c, panel 1). However, apoptosis signalling following Fas stimulation led to a significant decrease in this colocalization, with several areas around the plasma membrane showing an enhanced and distinct red fluorescence specific for the staining with anti-CL antibodies (Figure 1c, panel 2). Hence, confocal microscopy analysis confirmed previous findings[12] that Fas-mediated apoptosis was accompanied by early change in the intracellular distribution of immunoreactive CL molecules, which clustered around the plasma membrane while displaying a reduced colocalization with mitochondria.

Anti-CL reactivity and mitochondrial parameters during Fas-induced apoptosis

To complement the single-cell data with confocal microscopy, we carried out flow cytometry analysis using a variety of mitochondrial probes in combination with anti-CL staining and metabolic manipulation of intracellular processes (Figure 2). Cytofluorimetric analysis of surface staining with the affinity-purified human anti-CL antibodies showed a time-dependent reactivity of U937 cells (Figure 2a). The increase in cell surface staining with anti-CL IgG was evident after 20 min of Fas stimulation ($+68.6\pm5.2\%$) and was highly significant

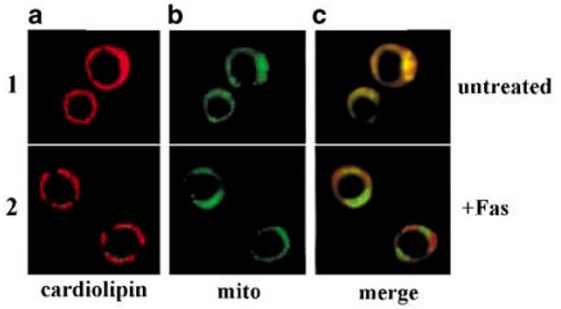

Figure 1 Confocal analysis of α-CL antibodies and Mito Tracker staining on the surface of U937 cells. U937 cells were directly stained with Mito Tracker Green FM for 2 h at 37°C; apoptosis was induced by incubating U937 cells (5×10^5/ml), with 100 ng/ml anti-Fas mAb for 1 h. Cells were permeabilized with ice-cold acetone and incubated with human affinity-purified anti-CL antibody for 1 h at 4°C and then with PE-conjugated anti-human IgG. The images were acquired with a scanning confocal microscope, collected at 512×512 pixels and processed with the Leica confocal software 4.7. Lane A1: untreated cells stained with anti-CL; lane A2: anti-CD95/Fas-treated cells stained with anti-CL; lane B1: untreated cells stained with Mito Tracker Green FM; lane B2: anti-CD95/Fas-treated cells stained with Mito Tracker Green FM; lane C1: dual immunolabelling of anti-CL and Mito Tracker Green FM in untreated cell; lane C2: dual immunolabeling of anti-CL and Mito Tracker Green FM in anti-CD95/Fas treated cells. Colocalization areas are stained in yellow

after 40 min of incubation ($+71.8\pm6.1\%$, $P<0.001$ *versus* control cells). This time course appeared comparable to that of PS exposure during death receptor-mediated apoptosis, as detected by Annexin V binding (Figure 2b). Interestingly, anti-CL staining was almost completely blocked by previous incubation of the cells with 20 μM nordihydroguaiaretic acid (NDGA) or 100 μM z-ValAlaAsp-fluoromethylketone (z-VAD-FMK) (Figure 2c). These findings strongly suggest that CL exposure on the cell surface is related to a complex process involving NDGA-sensitive enzymes, for instance lipoxygenases, as well as caspases. Activation of caspases is fundamental for PS exposure on the plasma membrane,[5–7] but the possible role of NDGA-sensitive reactions in the same process has not been documented before.

Owing to the predominant mitochondrial localization of CL[23] and its propensity to peroxidative damage following the increase in ROS associated with apoptosis induction,[21–26] we thought of interest to verify whether progressive exposure of CL on the cell surface correlated with extra production of mitochondrial ROS. Increase in the cellular level of ROS has been reported to occur early after activation of death receptors.[27] In this study, we used reduced Mito Tracker® red that detects with high-sensitivity ROS – including lipid hydroperoxides – produced by mitochondria,[27,28] but responds also to mitochondrial membrane potential, a parameter of mitochondrial function that is compromised during apoptosis progression.[3,22,25] Therefore, we complemented ROS measurements with TMRE, a probe that specifically responds to membrane potential.[28] ROS production progressively increased after Fas stimulation of U937 cells, with a log increase in Mito Tracker® fluorescence already after 40 min (Figure 2d, left panel). Incubation of cells with NDGA significantly decreased ROS production (Figure 2d), apparently correlating with the inhibition of anti-CL staining (Figure 2c). Under the same conditions, mitochondrial membrane potential was unaffected, either in the absence

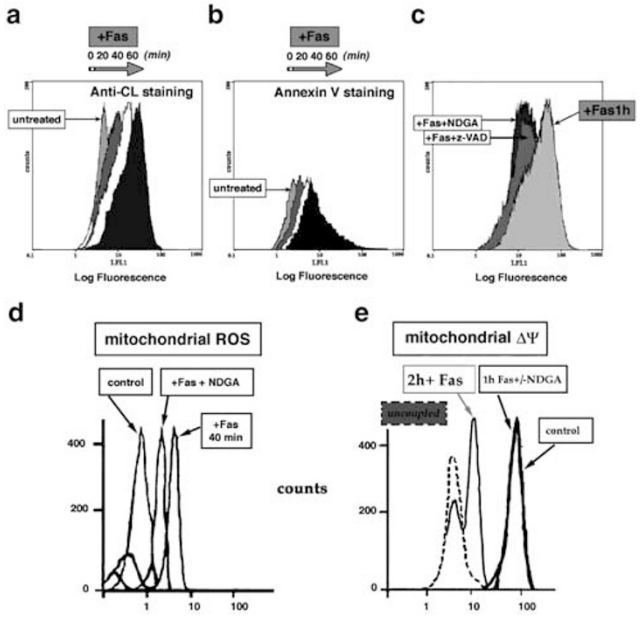

Figure 2 Cytofluorimetric analysis of anti-CL reactivity and mitochondrial parameters in anti-Fas-treated U937 cells. Apoptosis was induced by incubating the cells (5×10^5/ml) with anti-Fas (CD95) IgM mAb, 100 ng/ml for 0, 20 min, 40 min and 1 h. (**a–b**) Time course of CL expression on cell plasma membrane after treatment with anti-Fas. The cells were stained with affinity-purified aCL and subsequently incubated with FITC-conjugated goat anti-human IgG (**a**) or, alternatively, with FITC-conjugated Annexin V (**b**). Histograms represent log fluorescence *versus* cell number, gated on cell population of a side scatter/forward scatter (SS/FS) histogram. Cell number is indicated on the *y*-axis and fluorescence intensity is represented in three logarithmic units on the *x*-axis. (**c**) Specific inhibitors block exposure of CL on the surface of apoptotic cells. The figure shows cytofluorimetric analysis of U937 cells treated with anti-Fas agonist Ab for 1 h in the absence or presence of 20 μM NDGA or 100 μM z-VAD (see Materials and Methods). (**d**) Mitochondrial ROS production increases during Fas-induced death in U937 cells. The figure shows cytofluorimetric analysis of U937 cells treated for 40 min with anti-Fas agonist Ab in the absence or in the presence of 20 μM NDGA and subsequently loaded for 15 min with 500 nM reduced Mito Tracker Red® CM-H2XRos. (**e**) Membrane potential profile of mitochondria during Fas-induced death in U937 cells. The figure shows cytofluorimetric analysis of U937 cells treated with anti-Fas agonist for 1 or 2 h, in the absence or in the presence of preincubation with 20 μM NDGA, and subsequently loaded for 15 min with 40 nM TMRE. The dashed histogram refers to the data obtained after full uncoupling of membrane potential with the FCCP ionophore

or presence of NDGA (Figure 2e). TMRE fluorescence was barely affected up to 1 h of Fas stimulation, and clearly decreased only after 2 h of Fas stimulation (Figure 2e). At the same time, evident signs of cell death were detected, for example, DNA fragmentation.[12] Since we were interested to study the changes of mitochondrial CL that occurred early after Fas activation and before gross alteration of mitochondrial function, we subsequently restricted our studies to 1 h of Fas stimulation. Of note, z-VAD-FMK treatment had no significant effect on ROS production nor mitochondrial membrane potential up to 1 h after Fas stimulation (not shown).

MS analysis of membrane lipids in U937 cells

To provide an analytical basis to the intracellular distribution of CL that was detected with anti-CL antibodies (Figures 1 and 2 and Sorice[12]), we studied in detail the lipid composition of subcellular fractions obtained from untreated and Fas-activated U937 cells. After extraction of phospholipids using standard protocols,[19,20] we applied nanospray mass spectrometry (nanoES-MS) analysis in positive mode, which allows for recognition of minor species present in lipid extracts of cells and can resolve the various molecular forms of natural CL and their metabolites such as monolysocardiolipin, MCL.[29–31] The top panel in Figure 3a shows the characteristic ES-MS spectrum of a mitochondrial lipid extract from untreated (control) cells in the 1100–1600 mass-to-charge (*m/z*) range and illustrates the presence of multiple forms of MCL and CL.[31] Of note, standard lipid extraction with the Folch method[12,20,31] does not completely remove mitochondrial CL because of its avid binding to mitochondrial proteins. Consequently, MS profiles of mitochondrial lipids reflected the bulk of CL complement, the quantitative aspects of which could be evaluated with limited accuracy owing to the lack of appropriate molecular standards.

Our MS analysis identified various MCL species displaying substantial intensity in resting mitochondria (Figure 3), thereby underlining the physiological relevance of MCL in mitochondrial lipid remodelling.[8,23,31–34] This incompletely understood process[8,23] involves a continuous deacylation and reacylation of MCL intermediates that ensures maturation of newly synthesized CL, which is predominantly constituted by short and saturated fatty acids (e.g. tri-palmitoyl,oleoyl-2Na CL, 1424 *m/z* – present as a minor peak in Figure 3a), into its mature unsaturated forms like tri-linoleoyl,palmitoyl-3Na CL (1492 *m/z* – present as a major peak in Figure 3a) and tri-linoleoyl,oleoyl-3Na CL (1518 *m/z*) – see also references Degli Esposti *et al*.[31] and Xu *et al*.[34] These highly unsaturated species are predominant in the mitochondria of untreated U937 cells (Figure 3a, top panel), similarly to the distribution of CL species that is typical in mammalian heart and liver.[10,31]

Stimulation of Fas for 1 h induced a dramatic alteration of the MS profile in the CL region of mitochondrial lipid extracts, as shown in Figure 3a (second panel) and b. Most of the dominant CL species that were present in control mitochondria were not observed in the Fas-stimulated cells, with the notable exception of the peaks, 1464 and 1438 *m/z*, presumably corresponding with di-palmenyl,di-linoleoyl-3Na CL and tri-palmenyl,linoleoyl-3Na CL. Interestingly, the same CL species were detected also in the P100 fraction of both untreated and Fas-stimulated cells (Figure 3a, bottom panels), suggesting that they represented lipid molecules that resisted apoptosis-mediated degradation, possibly trafficking between different organelles. Their presence in fraction P100, which contained only a small proportion of mitochondria as verified by mitochondrial markers (see Figure 6 below), also indicated that these lipids could be formed (or actively remodelled) outside mitochondria. Of note, equivalent CL species have been reported to be predominant in mitochondria of Jurkat cells resistant to Fas-induced apoptosis.[20]

It was apparent that a considerable proportion of the CL species that had disappeared from the mitochondrial extract had been converted into corresponding MCL species, the level of which strongly increased in the mitochondrial extract of Fas-stimulated cells (Figure 3a). For instance, the two most intense peaks in the CL region of mitochondria from Fas-treated cells corresponded with peaks that could be attributed

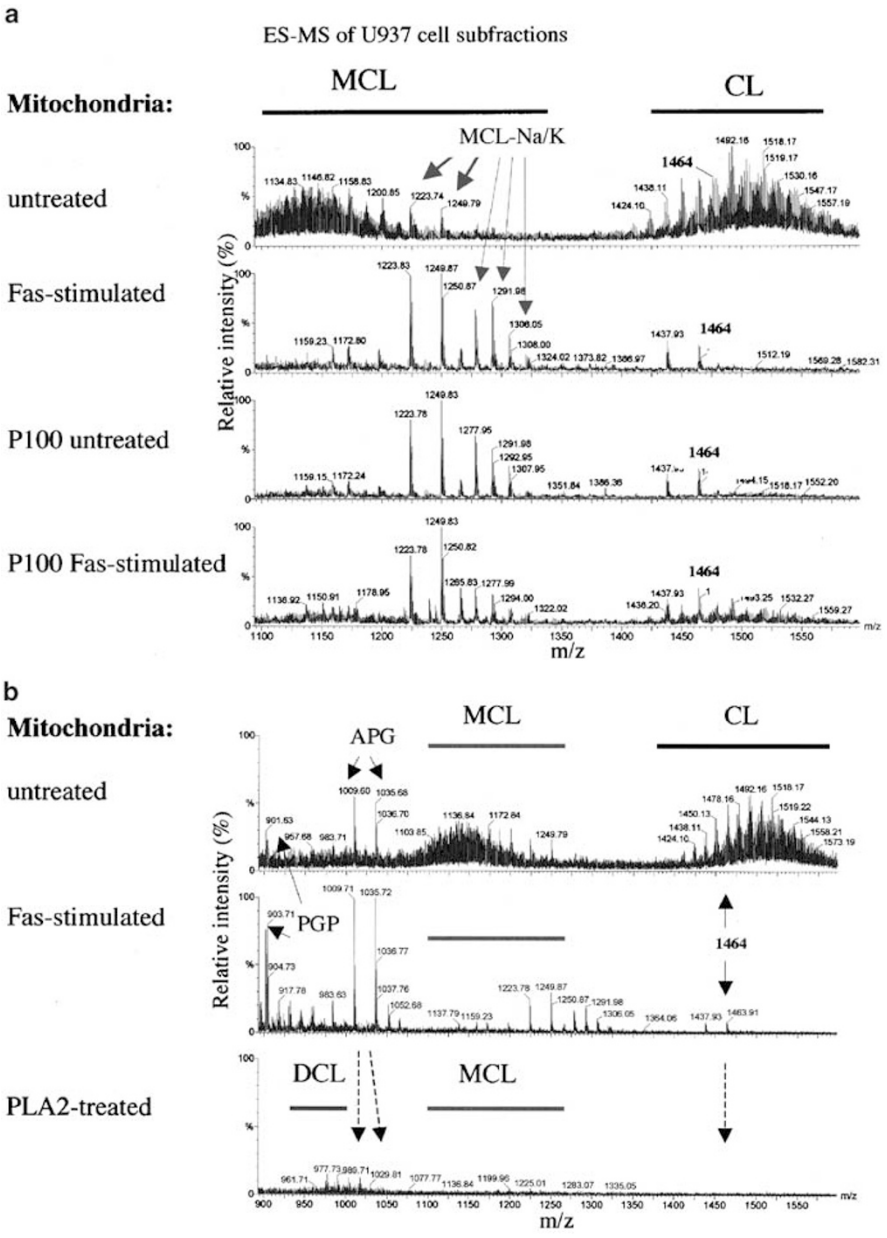

Figure 3 MS analysis of intracellular lipids before and after Fas stimulation of U937 cells. (**a**) The MS profile of lipid extracts from mitochondria (washed P10 fraction) and P100 fraction was analysed in positive mode. The lipid extracts were obtained from untreated and Fas-stimulated (1 h) U937 cells. Analysis was extended to the mass region encompassing all the MCL and CL species and the relative intensities are expressed in percentage *versus* the highest intensity peak. The content of phospholipids in the extract was very similar as determined from lipid phosphorus and internal standards. (**b**) Different MS profiles of mitochondrial lipids were observed after Fas stimulation and PLA2 treatment

to the sodium and potassium di-salt of tri-linoleoyl-MCL (1249 *m/z*) and di-linoleoyl,palmenyl-MCL (1223 *m/z*) (thick arrows in Figure 3a). These MCL species were present in low levels also in untreated cells, where the spectrum of other MCL species reflected the spread of mature CL species (Figure 3a, top panel). A similar pattern of CL decrease with parallel increase of derivative MCL species also occurred in mouse liver after Fas stimulation, but without strong peaks attributed to the potassium salts of CL metabolites[31] – presumably due to the limited availability of K in mitochondria isolated from primary tissues in comparison with those isolated from living cells. At difference with mouse liver, MS analysis indicated a profound and rapid loss of the major CL species present in mitochondria, even before major biochemical changes could be detected (Figures 1 and 3a). A principal reason for this difference is that transformed lymphoid cells, like U937, contain much less CL in their mitochondria than hepatocytes and other primary cells.[35] Consequently, U937 cells in culture may be much more tolerant to CL depletion than primary tissues – the damage that CL loss induces in oxphos enzymes being compensated by glycolysis, which is predominant in lymphoid cells of this kind. Moreover, our data suggest that CL loss in apoptotic mitochondria originates from conversion into MCL as well as redistribution to other organelles.

P100 fractions contained also MCL species that were not detected in control mitochondria, especially those corresponding to the peaks with 1278 and 1292 *m/z* (indicated by thin arrows in Figure 3a). These 'out of mitochondria' species could correspond with di-linoleoyl,arachidoyl-3Na MCL (1278 *m/z*), di-linoelyl,docosahexaenoyl–Na/K MCL (1292 *m/z*) and also di-oleoyl,docosahexaenoyl-3Na MCL (1306 *m/z*), which represent likely intermediates in the remodelling of CL species with poly-unsaturated fatty acids[32,33] (of note, docosahexaenoyl refers to a very long and unsaturated fatty acid, C22 : 6). Hence, the presence of significant levels of such MCL species in membranes other than those of mitochondria provided new direct evidence that CL metabolites are remodelled outside mitochondria in living cells, confirming earlier reports of efficient reacylation of lysocardiolipins in ER membranes.[32,33] Strikingly, Fas-mediated apoptosis produced a major alteration of the MCL profile in mitochondria but not in ER and other light membrane organelles. In fact, Fas stimulation induced only minor differences in the MCL profile of P100 fractions, contrary to mitochondria (Figure 3a).

CL may be converted into other negatively charged lipids during Fas-mediated apoptosis

We examined the following possibilities to explain the Fas-induced changes in the MS profile of cellular CLs (Figure 3a): (1) enhanced activation of mitochondrial phospholipase A2 (PLA-2); (2) increased hydroperoxidation; (3) conversion into other negatively charged lipids like PG or PI. To evaluate the first possibility, we compared the MS profile of mitochondrial lipid extract from Fas-treated cells with that of control mitochondria treated *in vitro* with PLA-2 and extended the analysis to the region encompassing the expected size of di-lysocardiolipin, DCL (Figure 3b). The MS profile of Fas-treated mitochondria (middle panel in Figure 3b) was completely different from that of PLA-2-treated mitochondria (bottom panel in Figure 3b). In particular, the dominant peaks of MCL salts were not observed in PLA-2-treated mitochondria, which conversely showed distinct peaks attributable to DCL species, for example 977 and 989 *m/z* (corresponding to oleoyl,linoleoyl-2Na DCL and di-oleoyl-Na/K DCL, respectively). These peaks had a reduced intensity, if any, in the mitochondrial extracts of untreated or Fas-stimulated cells (Figure 3b). Although these results were obtained with a harsh modification of mitochondrial lipids that may not represent a physiologically relevant situation, they suggested that the changes occurring after Fas stimulation were not comparable to those expected for an activation of endogenous PLA-2. Indeed, we could not detect an evident increase in the activity of mitochondrial PLA-2 (as well as in acidic PLAse of extra-mitochondrial fractions) after 1 h of Fas treatment of U937 cells, likewise in mouse liver.[31]

The second possibility was consistent with the increase in ROS production that was seen in U937 cells (Figure 2c). Owing to the strong effect of NDGA on these ROS (Figure 2c), we considered that NDGA-sensitive enzymes such as lipoxygenases could account, either directly or indirectly, for the degradation of CL that we observed by MS analysis. We thus stimulated cells and mouse liver with Fas agonist in the presence of NDGA concentrations that were effective in reducing ROS production (Figure 2) and compared the CL profile of mitochondrial lipid extracts with respect to those from cells and tissue treated with Fas agonists alone (Figure 4a). Clear results were obtained in mouse liver, in which over 50% inhibition of lipoxygenase activity (not shown) did not prevent CL conversion into MCL, which on the contrary appeared to increase with respect to Fas-treated mitochondria (Figure 4a). Hence, NDGA-sensitive enzymes like lipoxygenase, which might be responsible for lipid peroxidation during Fas-mediated apoptosis,[36] appeared not to be involved in the Fas-stimulated process of rapid degradation of mitochondrial CL. We also noted that NDGA treatment led to increased levels of other lipid species in mouse mitochondria (e.g. that with 960 *m/z*, Figure 4a), which were tentatively identified as Na salts of phosphorylated PI (PIP, see below). These inositides are normally associated with membrane traffic and NDGA is known to produce gross alteration of Golgi structure and traffic under the conditions used here[37] Consequently, the observed effects of NDGA may derive also from alteration of membrane traffic involving the Golgi apparatus.

The possibility that apoptosis enhanced the metabolism of negatively charged phospholipids was then explored in depth. It has been previously reported that apoptosis is associated with alteration in the metabolism of PG,[8,38] and in Jurkat T cells resistance to Fas-mediated death correlates with increased levels of PG in mitochondria.[20] Early work also showed that endo-lysosomal lipids like lyso-bis-phosphatidic acid (LBPA) and its acyl derivative semi-LBPA (SLBPA) redistributed in mitochondria during serum withdrawal – a model of apoptosis that was originally considered to produce 'cell degeneration'.[39,40] We thus evaluated whether increased levels of PG and/or LBPA could be detected in our subcellular fractions of Fas-stimulated cells. The prominent peak at 859.6 *m/z* that increased after Fas stimulation (Figure 4b,c) was initially considered to derive from the oleoyl,docosahexaenoyl-K species of either PG or LBPA.[41,42] However, the lipid species associated with this peak was strongly reduced after treatment with PLA-2 (Figure 3b), while LBPA is known to be resistant to PLA-2 degradation.[41] An increase in mitochondrial PI was also determined using TLC (not shown), which led to the possibility that the 859 *m/z* peak derived from a dominant PI species, palmitoyl,oleyl-Na (Figure 4b). After comparison with the published data of Han *et al.*,[43] we realized that the species 859 and 887 *m/z* may also correspond with triacylglycerol moieties.

Accumulation of triglycerides has been documented to occur in cells undergoing apoptosis or in pathological conditions associated with cell death.[43] Interestingly, our data suggested that the lipid(s) of the 859/887 *m/z* signature accumulated in mitochondria by redistribution from other cellular compartments, since the equivalent peak in fraction P100 correspondingly decreased after Fas stimulation (Figure 4b).

De novo biosynthesis of PI is linked to that of PG and CL by the common precursor diacylglycerol (DAG),[23] the concentration of which has been shown to increase during Fas signalling.[44,45] Indeed, after 1 h of Fas stimulation, we observed a significant increase in the basal levels of major

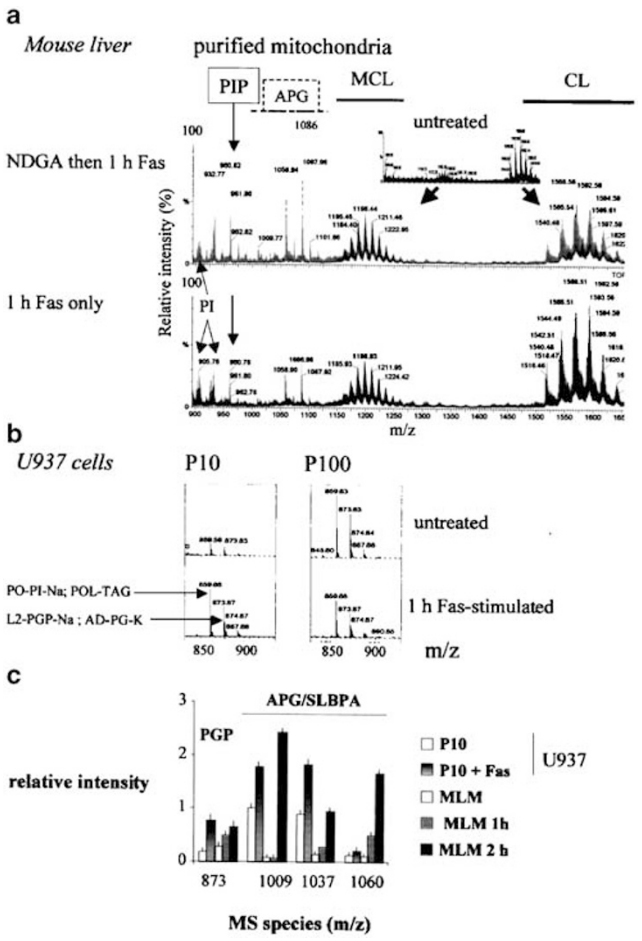

Figure 4 MS analysis of mitochondrial lipids after metabolic manipulation. (**a**) Mouse liver mitochondria were incubated *ex vivo* with Fas agonist Jo-2 mAb for 1 h either after preincubation with 20 μM NDGA (top panel) or the absence of the inhibitor (bottom panel). The inset shows the MS profile of untreated liver, cf. Degli Esposti *et al*.[31] (**b**) Changes in the relative intensity of the peaks attributed to negatively charged phospholipids plus triacyl-glycerols (TAG) were detected in various fractions of U937 cells. We envisage that the prominent peak 859 *m/z* that increased in fraction P10 after Fas stimulation derives from a mixture of PI (PO-PI-Na identifies the specific palmitoyl,oleoyl-species and POL-TAG, palmitoyl,linoleoyl,oleoyl-TAG, cf. Han *et al*.[43]), while the peak at 873 *m/z* derives from di-linoleoyl-PGP (L2-PGP-Na), possibly isobaric with either arachidoyl,docosanoyl-PG (AD-PG-K) or AD-LBPA-K. (**c**) Quantitative evaluation of PG derivatives was performed by MS analysis as in Figure 3 following the increase in the major peak with $m/z = 873$ and various APG/SLBPA species confirmed by fragmentation analysis (1009, 1036 and 1060 *m/z*, cf. (**a**) with respect to the internal reference of a CL species that changed little during Fas-mediated apoptosis in U937 cells, namely 1464 *m/z* (Figure 3a). For mouse liver mitochondria (MLM), the data were computed using a mixture of internal and external standards, and were normalized to the intensity of the tri-linoleoyl-oleoyl CL species, 1518 *m/z*, which was present in all lipid extracts (**a**). Results are the average of $n = 4$ measurements

DAG species with 581.4 *m/z* (stearoyl,palmitoyl) and 607.4 *m/z* (oleoyl,linoleoyl) in U937 cells, which mirrored a strong decrease in mitochondrial PC (but not PE, data not shown). These results would appear to be consistent with the reported increase in PC-PLC activity during death receptor-mediated cell death.[44,45] The activation of PLC could impact on CL remodelling by degrading it into DAG and phosphorylated PG (PGP), a transient intermediate of PG and CL biosynthesis.[23,46] In support of this, we noted the appearance or increase of MS signatures in the mitochondrial extract of Fas-stimulated cells that could be attributed to PGP species, in particular the peaks with 873 *m/z* (di-linoleoyl-Na PGP, Figure 4b) and 903 *m/z* (oleoyl,stearoyl-2Na PGP, Figure 3b, left). In both U937 cells and mouse liver, the increase in PGP species was restricted to mitochondria and appeared to level after 1 h of Fas activation (Figure 4b,c and data not shown), consistent with the intermediate nature of this lipid[23] and the transient stimulation of PGP synthase following apoptosis induction.[20]

Fas activation increases non-mitochondrial lipids in mitochondrial membranes

While focusing on the mass region encompassing PGP lipids, we realized that a diad of MS signatures with 960 *m/z* and 983 *m/z* that appeared after prolonged Fas activation could not be attributed to PG-related lipids. Following the recent description of PIP lipids in mouse cells,[47] these peaks were assigned to PIP species, either PI3P or PI4P with a complement of 36 : 4 acyl groups. PIP lipids are produced in various signalling pathways and are fundamental in endocytosis and membrane traffic,[47] but they have not been associated with mitochondrial fractions before, especially during cell death. However, the increase in PIP-attributable peaks was always preceded by the appearance of other prominent peaks in the 1000–1100 *m/z* region that could not be related to phosphorylated inositides, also because they showed a different digit and isotopic species distribution with respect to the 960/983 diad (Figure 4).

The novel MS peaks in the 1000–1100 *m/z* region have not been reported in mammalian cells before, but resembled the lipid species described as bacterial acyl-phosphatidylglycerol (APG).[48] APG are stereoisomers of SLBPA, an unusual lipid that has been reported to accumulate in mitochondrial fractions of dying cells[40] and to be present at significant levels in Golgi membranes.[49] Consistent with this observation, we noted that equivalent APG/SLBPA peaks appeared in the mitochondrial lipid extracts of liver and U937 cells early after Fas activation. After MS-MS analysis, we attributed these peaks to the following oleoyl species of APG: di-palmitoyl-Na (1009 *m/z*); palmitoyl,oleoyl-Na (1035 *m/z*); oleoyl,linoleoyl-Na (1058 *m/z*); di-oleoyl-Na (1060 *m/z*); and oleoyl,stearoyl-2Na (1086 *m/z*). The intensity of these APG/SLBPA lipids increased along the progression of Fas-induced apoptosis, especially after the increase in PGP species (Figure 4 and data not shown). The results obtained in mouse liver mitochondria (Figure 4a,c), which were much more purified that those obtained in U937 cells, confirmed that APG/SLBPA derivatives, that may function as LBPA precursors[41,50] had accumulated in mitochondrial membranes following Fas signalling. Indeed, this accumulation occurred concomitantly with the rapid degradation of CL (Figure 3), thereby suggesting that death signalling stimulated conversion of CL into (S)LBPA, as previously reported when mixing isolated mitochondria and lysosomes.[51] We also considered the possible alternative assignment of the 1009, 1035, 1060 *m/z* peaks to by-products of hydroperoxidative breakdown of MCL and CL, similar to those described in the lipids of Tangier

disease patients.[30] However, we excluded this alternative on the basis of the results obtained with NDGA treatment during Fas-mediated death, which increased the levels of the lipid species with 1009 and 1058 *m/z* (Figure 4a).

Independent confirmation of MS data was provided by chromatographic analysis of the phospholipid extract from both untreated and Fas-stimulated cells. In particular, HPTLC analysis revealed that the same spots containing CL in the extract of the P100 fraction were more prominent in cells treated with Fas than in control cells (Figure 5a). To ascertain this observation further, we refined the MS analysis in the CL region of P100 extracts (Figure 5b). Clearly, intermediate and mature CL species increased in fraction P100 of Fas-stimulated, but not untreated cells. These species included (Figure 5b): di-palmitoyl,di-oleoyl-2Na (1450 *m/z*) – an intermediate in remodelling that was clearly present in untreated mitochondria (Figure 3a); di-palmitoyl,oleoyl,linoleoyl-Na/K (1480 *m/z*); tri-linoleoyl,palmitoyl-3Na (1492 *m/z*) a most prominent species in the mitochondria of untreated cells (Figure 3a); di-linoelyl,oleoyl,palmitoyl-Na/K (1504 *m/z*); di-linoelyl,di-oleoyl-3Na (1520 *m/z*); and also significant traces of di-linoelyl,oleoyl,arachidoyl-3Na (1544 *m/z*) – a highly unsaturated CL species that rapidly disappears in mouse liver after Fas activation.[31] The presence of these CL species did not derive from an increased contamination of the P100 fraction with mitochondria, as documented by the comparable levels of Cox-IV, a specific marker of the inner mitochondrial membrane (Figure 5c). Consequently, redistribution of CL species to light membranes of other organelles was partially responsible for the loss of the same lipids in apoptotic mitochondria (Figure 3a). In Figure 5d we present a scheme, cf. Xu *et al*,[34] encompassing the observed changes in CL and related lipids.

Subcellular distribution of Bid and other proteins during Fas-mediated signalling

Studies with recombinant Bid indicated that its proapoptotic association with mitochondria could involve interaction with CL and its metabolites like MCL[18,31] Since we observed a relocation of CL on the plasma membrane of Fas-stimulated U937 cells,[19] as well as in fraction P100 (Figures 4 and 5), we investigated whether endogenous Bid showed comparable changes in its intracellular distribution after Fas stimulation of U937 cells. Although 1 h stimulation was insufficient for producing evident caspase cleavage of Bid into p15 tBid (cf. Degli Esposti *et al*.[31]), it induced a significant change in the intracellular distribution of full length (f.l.) Bid (Figure 6a). In untreated cells Bid was largely cytosolic, but associated in part also with membranes of either the P10 or P100 fraction (top panels in Figure 6a). After 1 h of Fas stimulation, the membrane association of Bid clearly increased, while its relative level in the cytosolic S100 fraction decreased (bottom panels in Figure 6a). Hence, Bid had redistributed from cytosol to membrane systems following Fas signalling in U937 cells, as previously found in mouse liver.[8,31]

Interestingly, Fas stimulation induced an increased association of Bid not only with the mitochondria-enriched fraction P10 but also with the light membranes of fraction P100, consistent with an increase of CL and its metabolites in the latter fraction (Figures 4 and 5). As P100 fractions contained other membrane systems associated with the cell surface, for instance endocytic vesicles, we could not exclude that the relocation of Bid observed after Fas stimulation derived in part from association to membrane vesicle systems close to, but not coincident with the plasma membrane. Considering also the reported internalization of Fas following ligation and activation,[52] we extended the characterization of our subcellular fractions to protein markers specific for the endocytotic pathway. Markers of endo-lysosomal organelles such as cathepsin D (Figure 6a) and Lamp-1 (M Degli Esposti, unpublished data) showed some increased presence in fraction P10 of Fas-treated cells, but in U937 cells this increase was limited and did not seem to correlate with lipid changes (e.g. unaltered distribution of LBPA), nor with a relative decrease in the content of mitochondrial markers like VDAC/porin (Figure 6a) and Cox IV (Figure 5c).

To verify whether the increased association of Bid with light membranes included also some relocation to the plasma membrane (i.e. is essentially contained within the P100 fraction), we isolated and purified plasma membranes in both untreated and anti-Fas-treated U937 cells as reported earlier.[12] Western blot analysis revealed that a band corresponding to f.l. Bid was clearly evident in Fas-stimulated cells, whereas no equivalent band was observed in the plasma membrane preparations from untreated cells (Figure 6b). Thus, it was found that Bid had relocated in part also to the plasma membrane following Fas activation and early death signalling, similarly to surface relocation of CL,[12] confirmed here using anti-CL antibodies (Figure 6c).

CL and MCL coimmunoprecipitate with Bid after induction of Fas-mediated apoptosis

Accumulating evidence indicates that Bid interacts with CL and its metabolites[8,17,18,31] However, demonstration that endogenous Bid binds to CL *in vivo* is lacking. Following our observations of a similar dynamic relocation of Bid and CL to intracellular membranes after Fas stimulation ((Figures 3–6), we tested whether association of Bid with CL could be verified by immunoprecipitation of the protein. Thus, we immunoprecipitated endogenous Bid from the P100 fraction of untreated and anti-Fas-treated cells and performed lipid extraction of the precipitated material. The phospholipids extracted from the Bid immunoprecipitates were then analysed by HPTLC followed by either iodide detection or anti-CL immunostaining. While no lipid was detected in control immunoprecipitates obtained with an irrelevant goat IgG (Figure 7a, lane 2), the immunoprecipitates from untreated cells contained only a very low level of CL (Figure 7a, lane 3), as verified by comigration with its standard. However, Bid immunoprecipitates from Fas-stimulated cells contained substantial levels of lipids, predominantly consisting of CL and MCL, as verified by TLC analysis (Figure 7a, lane 4) with respect to standards (Figure 7a, lane 1). TLC immunostaining with anti-CL antibodies further confirmed the identity of the lipid bands (not shown).

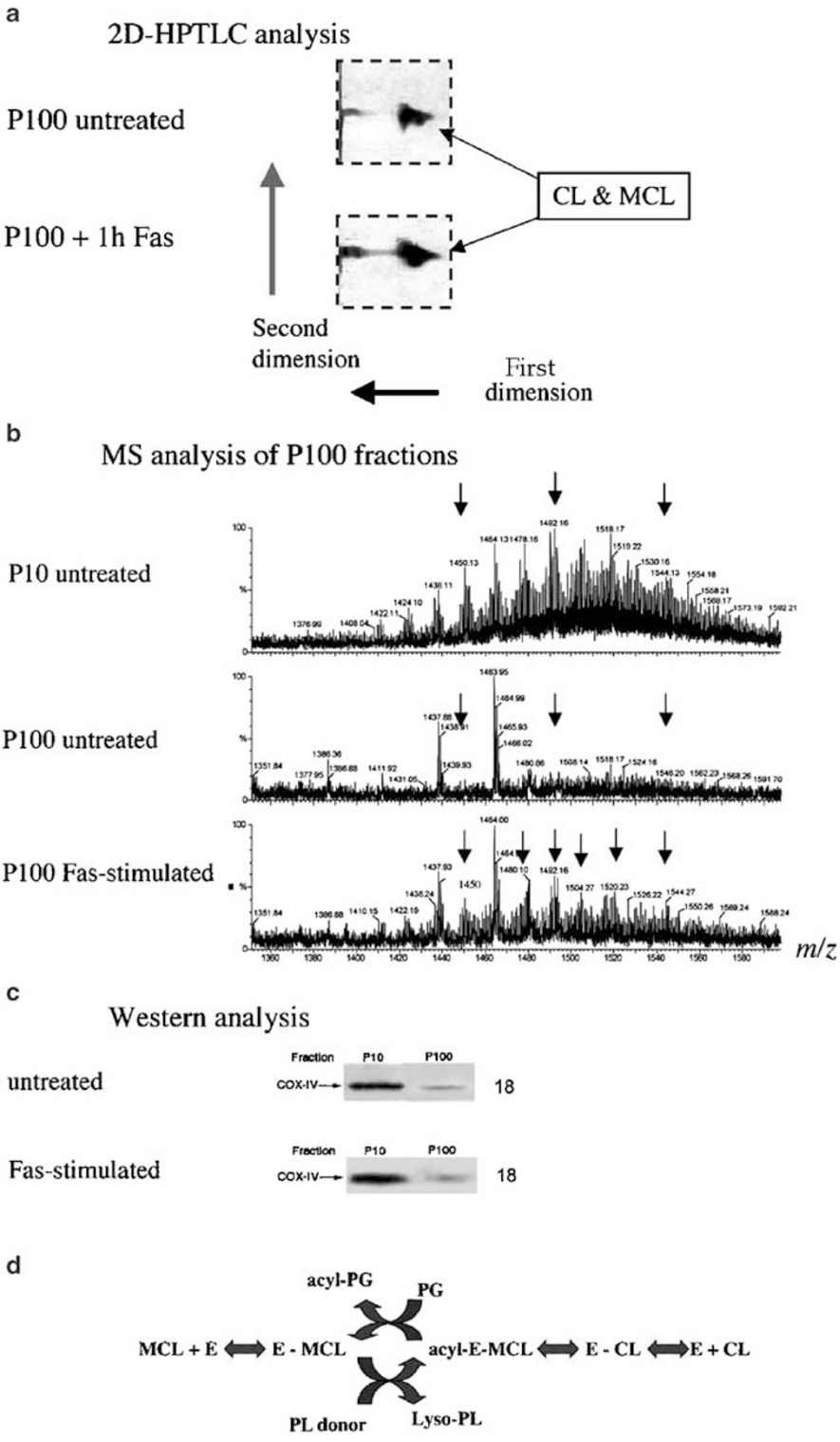

Figure 5 TLC *versus* MS analysis of intracellular lipids changes during Fas-induced apoptosis. (**a**) Separation of MCL and CL in fraction P100 extracts. Apoptosis was induced by incubating the cells (5×10^5/ml), with anti-Fas mAb for 1 h. Phospholipids were extracted from subcellular fractions and equal amounts of lipid phosphorus were separated by 2D-HPTLC as described in Materials and Methods. The panels show a section of the 2D-HPTLC containing the selected lipids. (**b**) MS profiling of the CL region in mitochondria (top panel) and P100 fraction before (middle panel) and after 1 h of Fas stimulation (bottom panel) evidences the increase of mature CL species in light membranes. The small arrows point to CL species that significantly increase in fraction P100 after Fas stimulation (see text). (**c**) Western blotting of fractions P10 and P100 was performed with a monoclonal antibody against subunit IV of cytochrome *c* oxidase (COX-IV), a specific marker of the inner mitochondrial membrane. (**d**) Proposed scheme of CL remodelling, adapted from Xu *et al*.,[34] including the novel lipids species observed here (Figures 3 and 4)

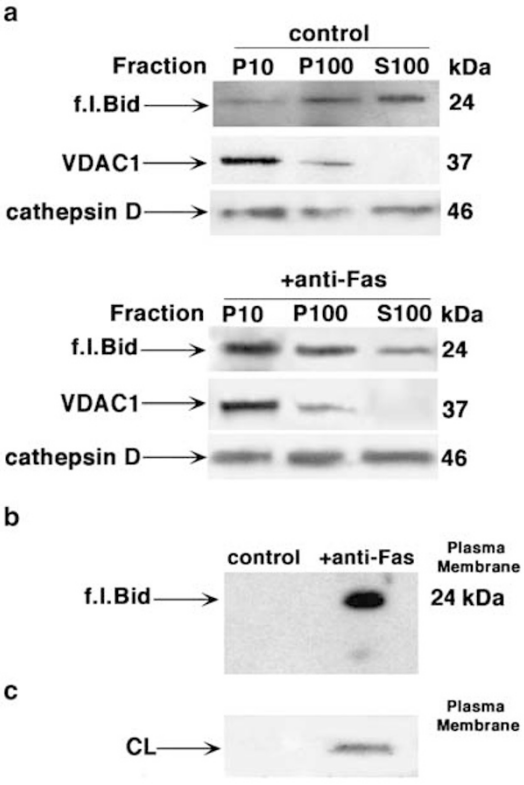

Figure 6 Bid redistributes between different intracellular membranes during Fas-induced apoptosis. (**a**) Detection of Bid in subcellular fractions of untreated or Fas-stimulated cells. P10, P100 and S100 fractions were separated by SDS-PAGE and probed with anti-Bid or with anti-VDAC/porin or anti-cathepsin D at 4°C overnight. (**b**) Detection of Bid in purified plasma membrane of untreated or Fas-stimulated cells. Equal protein loading of plasma membrane fractions were probed with anti-Bid at 4°C overnight. (**c**) The content of CL in the same fractions used in (**b**) was determined by immunodetection with purified anti-CL antibodies. On the basis of enzyme marker activities, the lysosomal and mitochondrial contaminations of the plasma membrane preparations were estimated to be 4.0 and 1.1%, respectively

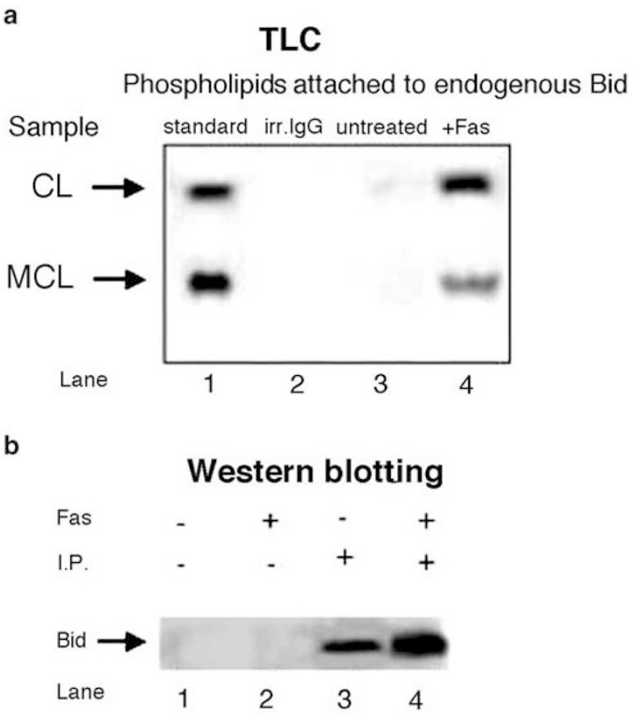

Figure 7 Bid immunoprecipitates contain increased levels of CL after CD95/Fas triggering. Detection of phospholipid molecules in the Bid immunoprecipitate. Fraction P100 from U937 cells, either untreated or Fas stimulated, was immunoprecipitated with an anti-Bid antibody. The immunoprecipitates were subjected to phospholipid extraction and analysed by monodimensional HPTLC analysis, followed by staining by exposure to iodide vapours. Lane 1, CL and MCL standard; lane 2, phospholipid extract of the immunoprecipitate obtained with an irrelevant IgG from Fas-treated cells; lane 3, phospholipid extract of Bid immunoprecipitate obtained from untreated cells; lane 4, phospholipid extract from the Bid immunoprecipitate obtained from Fas-treated cells. (**b**). Western blotting of Bid in immunoprecipitates obtained from fraction P100 as in (**a**); the unextracted precipitates were separated by SDS-PAGE and probed with the anti-Bid Ab at 4°C overnight. Lane 1, immunoprecipitate with an irrelevant IgG from untreated cells; lane 2, immunoprecipitate obtained with an irrelevant IgG from Fas-treated cells; lane 3, Bid immunoprecipitate from untreated cells; lane 4, Bid immunoprecipitate of Fas-treated cells as in (**a**)

Western blot analysis was conducted to verify the immunoprecipitation of Bid protein (Figure 7b). More Bid was present in the immunoprecipitate from the P100 fraction of Fas-stimulated than from that of untreated cells (Figure 7b), consistent with increased Bid association to light membranes following Fas stimulation (Figure 6a). However, the increase in the immunoprecipitated protein could not account for the much larger increase in coimmunoprecipitated CL nor for the presence of MCL, which was not detected in the immunoprecipitate of control cells (Figure 7a). Consequently, our results provide strong evidence supporting the concept that Bid interacts, *in vivo*, with CL and its metabolites like MCL.[31] Importantly, this interaction is strongly enhanced, either statically or dynamically, by Fas-mediated apoptosis.

Discussion

Although the fundamental aspects of cell death pathways are now outlined,[1] uncertainties remain in the identification of the early steps that are responsible for the involvement of mitochondria and other intracellular organelles following ligation of death receptors like Fas[2,45] Herein, we have used the so-called type II cells, in which Fas ligation inefficiently activates caspase 8 and mitochondria are required to amplify the caspase cascade through the release of apoptogenic factors.[1,2] Bid and other proteins of the Bcl-2 family are established regulators of death signalling and act directly on mitochondrial membranes to facilitate the release of apoptogenic factors.[1,53] Interaction with mitochondrial lipids, and especially CL, has been proposed to be instrumental in the proapoptotic action on mitochondria[8,17,53] and *in vitro* studies have sustained this view.[18,31,53] The present data contribute further *in vivo* evidence in support of the concept that Bid interacts with CL and its metabolites (Figure 7) while changing its intracellular distribution early after stimulation of Fas (Figure 6, cf. Degli Esposti *et al*.[17,31]) – and before gross perturbation of mitochondria (Figure 2). The parallel redistribution of mitochondrial CL and cytosolic Bid to the light membranes comprised in fraction P100 suggests a dynamic interaction of the protein with CL and its metabolites, consistent with the documented increase in the metabolism and

remodelling of CL and other lipids during apoptosis[20,23,31,38] and the lipid transferase activity of Bid.[17] Of particular significance is the finding that CL and MCL coimmunoprecipitate with Bid in Fas-stimulated cells (Figure 7) and that Bid relocates also to the plasma membrane (and/or associated membrane systems), likewise CL (Figure 6).

Our work provides novel evidence to advance the understanding of the traffic and remodelling of CL, a complex process of which we know very little at present. An early report[32] showed that both MCL and DCL were efficiently reacylated in microsomes (i.e. fraction P100), while later works reported that MCL reacylation is also undertaken by isolated mitochondria,[10,33,34] where the native lipid is synthesized via DAG and PGP precursors.[23] The fact that CL synthase is restricted to the inner mitochondrial membrane[10,23] has led to the common assumption that CL is associated only with this membrane[23,26] However, active remodelling of nascent CL into its mature, highly unsaturated forms that are predominant in tissues and cells (Figures 3 and 5B, cf. McMillin and Dowhan,[23] Eichberg,[32] Schlame and Rustow,[33] and Xu *et al*.[34]) fundamentally occurs in the outer membrane, where it could be transferred by a phospholipid scramblase.[54] In addition, CL translocation to the outer mitochondrial membrane may involve an increase in the rate of transbilayer diffusion, promoted by an activated form of Bax, as observed in artificial liposomes.[55] Moreover, CL degradation occurs efficiently in lysosomes,[23,56] where it provides the precursors for the biosynthesis of LBPA.[50,51]

Our novel MS data indicate that substantial levels of MCL are present in the light membranes of fraction P100 of U937 cells, where limited contamination by inner membrane components was detected (Figures 5d and 6a and data not shown). Increased levels of mature CL species were also observed in this fraction after 1 h of Fas stimulation (Figure 5b), concomitantly with an increase of non-mitochondrial lipids like APG/SLBPA (and PIP) in the mitochondria-rich fraction P10 (Figure 4). Of note, the surface exposure of CL and MCL in Fas-treated cells shows similarity with that recently described for the phospholipid-binding protein annexin I in Jurkat T cells, which is also blocked by z-VAD.[6,57] Blocking caspases with a broad spectrum inhibitor like z-VAD might interfere with the normal traffic of membranes that is responsible for rearrangement of the plasma membrane and associated endocytic vesicles, as documented for the Fas receptor itself.[52]

Detailed studies with specific membrane markers showed some redistribution or mixing of extra-mitochondrial organelles with mitochondria, for example, enhanced levels of Lamp-1 were detected in fraction P10 after Fas stimulation in mouse liver (M Degli Esposti, unpublished results). However, in U937 cells, the substantial changes in membrane lipids such as the appearance of APG/SLBPA species in mitochondria were more significant that those expected from the limited contaminations by endo-lysosomal membranes, suggesting the participation of catalytic processes. We are currently investigating these catalytic processes linking CL degradation to SLBPA biosynthesis in order to identify the enzyme(s) responsible, and also to verify potential connections with the endocytic traffic of vesicles that could be stimulated by Fas activation.[2,3,31,52,58]

Materials and Methods

Cells culture and apoptosis induction

Human pro-monocytic U937 cells were cultured in RPMI 1640 medium (Gibco-BRL, Life Technologies Italia, Milano, Italy) containing 10% foetal calf serum (FCS) at 37°C in a humified 5% CO_2 atmosphere. Apoptosis was induced by incubating cells at a concentration of 5×10^5 per ml in a serum-free medium supplemented with insulin (5 μg/l) and transferrin (5 μg/l), and by adding anti-Fas (CD95) IgM MoAb (clone CH11, Upstate Biotechnology, Lake Placid, NY, USA) at 100 ng/ml for up to 2 h, as described previously.[12] After treatment, cells were collected and prepared for other procedures as described below.

Antibodies

Human anti-CL (IgG αCL) antibodies were purified by affinity chromatography from a patient with the APS, according to McNeil *et al*.,[59] and were selected on the basis of their specific binding to CL, as demonstrated by TLC immunostaining.[12,19] Reactivity showed specificity for CL and MCL, since no significant reaction was detected with other negatively charged lipids like PS and phosphatidylinositol (PI), nor with LBPA or β_2-glycoprotein I. Affinity-purified normal human IgG (from blood donors) were used as a control. Commercial antibodies for Bid, cathepsin D, EEA1, Lamp1, cytochrome *c* and subunit IV of cytochrome oxidase were obtained from R&D Systems Inc. (Minneapolis, MN, USA), Santa Cruz Biotechnologies (Santa Cruz, CA, USA), Upstate Biotechnologies (Lake Placid, NY, USA), BD-PharMingen and Molecular Probes (Eugene, OR, USA).

Analysis of CL localization by scanning confocal microscopy

U937 cells were directly stained with Mito Tracker Green FM (Molecular Probes) for 2 h at 37°C and then stimulated with Fas for 1 h at 37°C, as reported above. Both untreated and Fas-stimulated cells were stained for anti-CL antibodies with a protocol involving permeabilization with ice-cold acetone, soaking in balanced salt solution (BSS) (Sigma, St Louis, MO, USA) and blocking with 2 % BSA in PBS.[12] After washing three times with PBS, cells were incubated for 1 h at 4°C with either human purified IgG αCL or with control human IgG in PBS containing 1% BSA. Phycoerythrin (PE)-conjugated anti-human IgG (Jackson ImmunoResearch, West Grove, PA, USA) were then added and incubated at 4°C for 30 min. In parallel experiments, cells were stained with purified IgG αCL before fixation. Fixation procedures did not affect CL staining on the cell surface.[12] After incubation, the cells were washed three times with PBS and then resuspended in 0.1 M Tris-Cl, pH 9.2, containing 60% glycerol (v : v). The images were acquired with a Leica TCS SP2 confocal laser scanning microscope, usually with a $\times$ 40 objective. Acquisition of single FITC-stained samples in dual fluorescence scanning configuration did not show contribution of green signal in red. Images were collected at 512×512 pixels and processed with the Leica confocal software 4.7.

Immunofluorescence and flow cytometric analysis

Indirect immunofluorescence was used to visualize CL on the plasma membrane of U937 cells. Samples of 10^6 cells/ml were incubated in the presence of 20 μM of the lipoxygenase inhibitor NDGA (Sigma)[60] or 100 μM of the pan-caspase inhibitor *N*-benzyloxycarbonyl-Val-Ala-Asp-fluoromethyl ketone (z-VAD-fmk) (Calbiochem)[61] for 15 min before

treatment with anti-Fas for 20–120 min, and subsequently divided in aliquots for parallel staining with anti-CL antibodies and mitochondrial markers. For CL staining, cells were fixed in PBS containing 4% formaldehyde for 1 h at 4°C. After washing three times with PBS, cells were incubated with human purified IgG αCL for 1 h at 4°C. PS exposure was measured directly by the binding of FITC-conjugated Annexin V using the Apoptest binding kit, containing annexin V-FITC and binding buffer. Fluorescence intensity was analysed with an Epics XL-MCL cytometer (Coulter Electronics, Hialeah, FL, USA), as previously reported.[12] In separate experiments, cells were directly stained with anti-CL antibodies before fixation. For mitochondrial markers, cells were washed in PBS and subsequently loaded with either 40 nM tetramethyl-rhodamine-ethyl-ester (TMRE) or 500 nM reduced Mito Tracker Red® CM-H2XRos (both from Molecular Probes) for 15 min, as described.[28]

Subcellular fractions

Subcellular fractions were isolated from U937 cells essentially as previously reported.[17] Control untreated cells and cells treated with the agonist anti-Fas antibody (100 ng/ml for 1 h) were rinsed with cold isolation buffer (0.25 M Mannitol, 1 mM EDTA, 10 mM K-Hepes, 0.2% BSA, pH 7.4) containing a cocktail of protease inhibitors (Sigma), resuspended in 1 ml of the same buffer and homogenized vigorously. After a brief centrifugation at $600 \times g$ in the cold, pellet and supernatant were combined, rehomogenizated and centrifuged at $800 \times g$ for 10 min at 4°C. The pellet was discarded and the supernatant was further centrifuged at $10\,000 \times g$ for 10 min at 4°C. The pellets (P10) were washed three times with assay buffer (0.12 M Mannitol, 0.08 M KCl, 1 mM EDTA, 20 mM K-Hepes, pH 7.4, containing a cocktail of protease inhibitors) and then resuspended in the same buffer. The supernatant was further centrifuged at $100\,000 \times g$ for 1 h at 4°C to obtain the cytosolic supernatant (S100) and the light membrane pellet (P100), which was dissolved in assay buffer. Mouse liver was Fas activated with the Jo-2 agonist antibody (BD-PharMingen) and subfractionated as described previously.[17] Fractions were stored at –70°C until processed for phospholipid analysis and Western blotting.

Plasma membrane fraction from U937 cells was isolated by sucrose gradient centrifugation as reported previously.[12,62] The purity of plasma membrane preparations was evaluated with enzyme marker activities,[62] including nucleotidase and alkaline phosphodiesterase that showed about 45-fold enrichment compared with the whole homogenate.[12] On the contrary, NADPH-cytochrome *c* reductase and glucose-6-phosphatase showed a significant decrease of their specific activities in the plasma membrane fraction compared to the initial homogenate – not shown, cf. Sorice *et al*.[12] As a routine marker of mitochondria, we used the specific assay of cytochrome oxidase following ferrocytochrome *c* oxidation.[28] The same marker enzymes were used, together with Western blotting, to verify the relative content of plasma membrane, ER, endo-lysosomes and mitochondria in the various subcellular fractions, the protein content of which was measured with the Bio-Rad protein assay.[17]

Lipid extraction and analysis by MS

Extraction of lipids from subcellular fractions was undertaken with chloroform:methanol[20,63] as follows. In total, 2–5 mg of any subcellular fraction was treated with 1 ml methanol and subsequently with 2 ml of chloroform. After vigorous mixing for 5 min, samples were further mixed with 0.5 ml of 0.15 M NaCl[20] and the organic phase was separated by centrifugation, dried under nitrogen, dissolved in chloroform, and recentrifuged to remove any insoluble material. Phospholipids were separated using high-performance thin layer chromatography (HPTLC) with silica gel plates 10×10 cm (Merck, Darmstadt, Germany).[12,19] The HPTLC plates were developed in the first dimension with a solvent system of chloroform/methanol/ammonium hydroxide (80 : 20 : 2, v/v/v), and in the second dimension with a solvent system containing propanol/water/acetic acid (80 : 10 : 10; v/v/v), as reported in referenece Fischer *et al*.[64] Lipids were stained by exposure to iodide vapours.[12,19]

Detailed analysis of the lipids extracted from subcellular fractions was carried out by nanospray – Time-of-flight (ToF) mass spectrometry essentially as described earlier.[29–31,43,65,66] Analyses were performed on a Q-ToF I instrument (Micromass, Manchester, UK). A volume of 2–4 μl from each sample was introduced into the mass spectrometer in nanospray gold-coated needles (Micromass). The instrument settings for the MS mode were the following: capillary potential 900 V, sample cone 47 V, extractor 0 V, and collision offset 4 V. The MS data were acquired in continuum mode over the range of 100–2000 *m/z*. All data were acquired and processed using MassLynx v.3.4 software. For comparative analysis, we used both nonphysiological lipids such as Bis-BODIPY FL®C_{11}-PC and endogenous lipids that were found to remain essentially unaltered either after prolonged Fas-induced apoptosis or treatment with phospholipase A2, for example, palmitoyl-SM, $m/z = 703.6$ in its protonated form.[31]

Western blot analysis of Bid distribution in subcellular fractions

Subfractions or whole-cell lysates were diluted with assay buffer containing protease inhibitors and adjusted to a final protein concentration of 0.5–1 mg/ml with concentrated SDS-sample buffer. Protein samples (usually 20 μg/ml) were separated by SDS-polyacrilamide gel electrophoresis (SDS-PAGE) and blotted in PBS containing 0.05% Tween-20 (PBST) with anti-Bid (R&D Systems AF860) at 4°C overnight, or, as subcellular markers, with anti-VDAC/porin (N18 Santa Cruz Biotechnologies), anti-cathepsin D, anti-Cox IV and a monoclonal anti-transferrin receptor (a kind gift of Phil Woodman, University of Manchester), as reported previously.[17] Blots were visualized by chemiluminescence reaction, using the ECL Western detection system (Amersham Biosciences). Protein loading was evaluated also by India ink staining.[67]

Detection of lipids in Bid immunoprecipitates

Since a considerable proportion of endogenous Bid is associated with light membranes,[17] we used the P100 fraction to determine whether specific lipids coimmunoprecipitated with the Bid protein. P100 fraction from untreated or anti-Fas-treated cells (about 1.5×10^8) were resuspended in a buffer containing 20 mM Tris-Cl, pH 7.5, 0.15 M NaCl, 1 mM EDTA, 0.02% NaN_3, 10 mM NaF, 1 mM Na-ortho-vanadate, 0.25 mM PMSF, 1 μg/ml aprotinin, 1 μg/ml leupeptin and 1 μg/ml chymostatin. The mixtures were rocked at 4°C for 30 min and, after a brief centrifugation at $3000 \times g$ for 5 min to remove insoluble material, were precleared with Protein G-sepharose (Sigma) by centrifugation at $12\,000 \times g$ for 30 s and then incubated with 10 μg of goat anti-Bid (R&D Systems) per mg of protein for 2 h at 4°C. At the end of the incubation, protein G-sepharose (Sigma) was added and the mixture was rocked in the cold for an additional 1 h. As a negative control, immunoprecipitation was performed with an irrelevant goat IgG (from Sigma). A major portion of the immunoprecipitate was subjected to phospholipid extraction according to the method of Folch[63] and separated by HPTLC in a single dimension by using a solvent system of chloroform/methanol/acetic acid/water

(100 : 75 : 7 : 4, v/v/v/v). Phospholipids were stained by exposure to iodide vapours and also immunostained with the purified human αCL IgG as previously reported.[12] In order to check the immunoprecipitation of endogenous Bid from the subcellular fraction, an aliquot of the immunoprecipitate was separated by electrophoresis and Western blotted as above.

Acknowledgements

The work in Rome was supported by MIUR, and a grant to M Sorice. Research in Manchester has been sponsored by AICR and Barth Syndrome Foundation, Inc. We warmly thank Simon Gaskell and Caroline Dive for their support and Ying Chen for technical assistance.

References

1. Green DR, Droin N and Pinkoski M (2003) Activation-induced cell death in T cells. Immunol. Rev. 193: 70–81
2. Jaattela M and Tschopp J (2003) Caspase-independent cell death in T lymphocytes. Nat. Immunol. 4: 416–423
3. Boya P, Andreau K, Poncet D, Zamzami N, Perfettini JL, Metivier D, Ojcius DM, Jaattela M and Kroemer G (2003) Lysosomal membrane permeabilization induces cell death in a mitochondrion-dependent fashion. J. Exp. Med. 197: 1323–1334
4. Peitsch MC, Mannhers HG and Tschopp J (1994) The apoptosis endonucleases: cleaning up after cell death? Trends Cell Biol. 4: 37–41
5. Martin SJ, Reutelinsperger CPM, McGahon AJ, Rader JA, van Schie RCAA, LaFace DM and Green DR (1995) Early redistribution of plasma membrane phosphatidylserine is a general feature of apoptosis regardless of the initiating stimulus: inhibition by overexpression of Bcl-2 and Abl. J. Exp. Med. 182: 1545–1556
6. Fadok VA and Henson PM (2003) Apoptosis: giving phosphatidylserine recognition an assist – with a twist. Curr. Biol. 13: 655–657
7. Verhoven B, Schlegel RA and Williamson P (1995) Mechanisms of phosphatidylserine exposure, a phagocyte recognition signal on apoptotic T lymphocytes. J. Exp. Med. 182: 1597–1601
8. Degli Esposti and M (2002) Lipids, cardiolipin and apoptosis: a greasy licence to kill. Cell Death Differ. 9: 234–236
9. Bretsche MS (1972) Asymmetrical lipid bilayer structure for biological membranes. Nature 236: 11–12
10. Schlame M, Rus D and Greenberg ML (2000) The biosynthesis and functional role of cardiolipin. Prog. Lipid Res. 39: 257–288
11. Fernandez MG, Troiano L, Moretti L, Nasi M, Pinti M, Salvioli S, Dobrucki J and Cossarizza A (2002) Early changes in intramitochondrial cardiolipin distribution during apoptosis. Cell Growth Differ. 13: 449–455
12. Sorice M, Circella A, Misasi R, Pittoni V, Garofalo T, Cirelli A, Pavan A, Pontieri GM and Valesini G (2000) Cardiolipin on the surface of apoptotic cells as possible trigger for antiphospholipid antibodies. Clin. Exp. Immunol. 122: 277–284
13. Luo X, Budihardjo I, Zou H, Slaughter C and Wang X (1998) Bid, a Bcl2 interacting protein, mediated cytochrome *c* release from mitochondria in response to activation of cell death receptors. Cell 94: 481–490
14. Wei MC, Lindsen T, Mootha VK, Eiler S, Gross A, Ashiya A, Thompson CB and Korsmeyer SJ (2000) tBID, a membrane-targeted death ligand, oligomerizes BAK to release cytochrome *c*. Genes Dev 10: 2060–2071
15. Yin XM, Wang K, Gross A, Zhao Y, Zinkel S, Klocke B, Roth KA and Korsmeyer SJ (1999) Bid-deficient mice are resistent to Fas-induced hepatocellular apoptosis. Nature 400: 886–891
16. Zha J, Weiler S, Oh K, Wei MC and Korsmeyer SJ (2000) Posttranslational N-myristoylation of BID as a molecular switch for targeting to mitochondria and apoptosis. Science 290: 1761–1765
17. Degli Esposti M, Erler JT, Hickman JA and Dive C (2001) Bid, a widely expressed proapoptotic protein of the Bcl-2 family, displays lipid transfer activity. Mol. Cell. Biol. 21: 7268–7276
18. Lutter M, Fang M, Luo X, Nashijima M, Xie X and Wang X (2000) Cardiolipin provides specificity for targeting of tBid to mitochondria. Nat. Cell Biol. 2: 754–756
19. Sorice M, Griggi T, Circella A, Garofalo T, d'Agostino F, Pittoni V, Pontieri GM, Lenti L and Valesini G (1994) Detection of antiphospholipid antibodies by immunostaining on thin layer chromatography plates. J. Immunol. Methods 173: 49–54
20. Matsko CM, Hunter OC, Rabinowich H, Lotz, MT and Amoscato AA (2001) Mitochondrial lipids alterations during Fas- and radiation-induced apoptosis. Biochem. Biophys. Res. Commun. 287: 1112–1120
21. Nomura K, Imai H, Koumura T, Kobayashi T and Nakagawa Y (2000) Mitochondrial phospholipid hydroperoxide glutathione peroxidase inhibits the release of cytochrome *c* from mitochondria by suppressing the peroxidation of cardiolipin in hypoglycaemia-induced apoptosis. Biochem. J. 351: 183–193
22. Kirkland RA, Adibhatla RM, Hatcher JF and Franklin JL (2002) Loss of cardiolipin and mitochondria during programmed neuronal death: evidence for a role for lipid peroxidation and autophagy. Neuroscience 115: 587–602
23. McMillin JB and Dowhan W (2002) Cardiolipin and apoptosis. Biochim. Biophys. Acta 1585: 97–107
24. Hockenbery DM, Oltvai ZN, Yin XM, Milliman CL and Korsmeyer SJ (1993) Bcl-2 functions in an antioxidant pathway to prevent apoptosis. Cell 75: 241–251
25. Macho A, Castedo M, Marchetti P, Aguilar JJ, Decaudin D, Zamzami N, Girard PM, Uriel J and Kroemer G (1995) Mitochondrial dysfunctions in circulating T lymphocytes from human immunodeficiency virus 1 carriers. Blood 86: 2481–2487
26. Ott M, Robertson JD, Gogvadze V, Zhivotosky B and Orrenius S (2002) Cytochrome *c* release from mitochondria proceeds by a two-steps process. Proc. Natl. Acad. Sci. USA 99: 1259–1263
27. Degli Esposti M, Hatzinisiriou I, McLennan H and Ralph S (1999) Bcl-2 and mitochondrial oxygen radicals. New approaches with reactive oxygen species-sensitive probes. J. Biol. Chem. 274: 29831–29837
28. Degli Esposti M (2001) Assessing functional integrity of mitochondria *in vitro* and *in vivo*. Methods Cell. Biol. 65: 75–96
29. Schaffer C, Beckedorf AI, Scheberl A, Zayni S, Peter-Katalinic J and Messner P (2002) Isolation of glucocardiolipins from Geobacillus stearothermophilus NRS 2004/3a. J. Bacteriol. 184: 6709–6713
30. Fobker M, Voss R, Reinecke H, Corne C, Assmann G and Walter M (2001) Accumulation of cardiolipin and lysocardiolipin in fibroblasts from Tangier disease subjects. FEBS Lett. 500: 157–162
31. Degli Esposti M, Cristea IM, Gaskell SJ, Nakao Y and Dive C (2003) Pro-apoptotic Bid binds to monolysocardiolipin, a new molecular connection between mitochondrial membranes and cell death. Cell Death Differ. 10: 1300–1309
32. Eichberg J (1974) The reacylation of deacylated derivatives of diphosphatidylglycerol by microsomes and mitochondria from rat liver. J. Biol. Chem. 249: 3423–3429
33. Schlame M and Rustow B (1990) Lysocardiolipin formation and reacylation in isolated rat liver mitochondria. Biochem. J. 272: 589–595
34. Xu Y, Kelley RI, Blanck TJ and Schlame M 2003 Remodeling of cardiolipin by phospholipid transacylation. J. Biol. Chem. 278: 51380–51385
35. Morton R, Cunningham C, Jester R, Waite M, Miller N and Morris HP (1976) Alteration of mitochondrial function and lipid composition in Morris 7777 hepatoma. Cancer. Res. 36: 3246–3254
36. Wagenknecht B, Gulbins E, Lang F, Dichgans J and Weller M (1997) Lipoxygenase inhibitors block CD95 ligand-mediated apoptosis of human malignant glioma cells. FEBS Lett. 409: 17–23
37. Drecktrah D, de Figueiredo P, Mason RM and Brown WJ (1998) Retrograde trafficking of both Golgi complex and TGN markers to the ER induced by nordihydroguaiaretic acid and cyclofenil diphenol. J. Cell Sci. 111: 951–965
38. Ostrander DB, Sparagna GC, Amoscato AA, McMillin JB and Dowhan W (2001) Decreased cardiolipin synthesis corresponds with cytochrome *c* release in palmitate-induced cardiomiocyte apoptosis. J. Biol. Chem. 276: 38061–38067
39. Brotherus J and Renkonen O (1977) Phospholipids of subcellular organelles isolated from cultured BHK cells. Biochim. Biophys. Acta 486: 243–253
40. Somerharju P (1979) Subcellular localization of three degeneration-associated phospholipids in cultured hamster fibroblasts (BHK21 cells). Biochim. Biophys. Acta 574: 461–470

41. Kobayashi T, Beuchat MH, Chevallier J, Makino A, Mayran N, Escola JM, Lebrand C, Cosson P, Kobayashi T and Gruenberg J (2002) Separation and characterization of late endosomal membrane domains. J. Biol. Chem. 277: 32157–32164
42. Luquain C, Dolmazon R, Enderlin JM, Laugier C, Lagarde M and Pageaux JF (2000) Bis(monoacylglycerol) phosphate in rat uterine stromal cells: structural characterization and specific esterification of docosahexaenoic acid. Biochem. J. 351: 795–804
43. Han X, Abendschein DR, Kelley JG and Gross RW (2000) Diabetes-induced changes in specific lipid molecular species in rat myocardium. Biochem. J. 352: 79–89
44. Cifone MG, Roncaioli P, De Maria R, Camarda G, Santoni A, Ruberti G and Testi R (1995) Multiple pathways originate at the Fas/APO-1 (CD95) receptor: sequential involvement of phosphatidylcholine-specific phospholipase C and acidic sphingomyelinase in the propagation of the apoptotic signal. EMBO J. 14: 5859–5868
45. Degli Esposti M (2003) The mitochondrial battlefield and membrane lipids during cell death signalling. Ital. J. Biochem. 52: 43–50
46. Xu FY, Kelly SL, Taylor WA and Hatch GM (1998) On the mechanism of the phospholipase C-mediated attenuation of cardiolipin biosynthesis in H9c2 cardiac myoblast cells. Mol. Cell. Biochem. 188: 217–223
47. Wenk MR, Lucast L, Di Paolo G, Romanelli AJ, Suchy SF, Nussbaum RL, Cline GW, Shulman GI, McMurray W and De Camilli P (2003) Phosphoinositide profiling in complex lipid mixtures using electrospray ionization mass spectrometry. Nat. Biotechnol. 21: 813–817
48. Yague G, Segovia M and Valero-Guillen PL (1997) Acyl phosphatidylglycerol: a major phospholipid of Corynebacterium amycolatum. FEMS Microbiol. Lett. 151: 125–130
49. Cluett EB, Kuismanen E and Machamer CE (1997) Heterogeneous distribution of the unusual phospholipid semilysobisphosphatidic acid through the Golgi complex. Mol. Biol. Cell. 8: 2233–2240
50. Waite M, King L, Thornburg T, Osthoff G and Thuren TY (1990) Metabolisms of phosphatidylglycerol and bis(monoacylclycerol)-phosphate in macrophage subcellular fractions. J. Biol. Chem. 265: 21720–21726
51. Poorthuis BJ and Hostetler KY (1978) Conversion of diphosphatidylglycerol to bis(monoacylglyceryl)phosphate by lysosomes. J. Lipid Res. 19: 309–315
52. Algeciras-Schimnich A, Shen L, Barnhart BC, Murmann AE, Burkhardt JK and Peter ME (2002) Molecular ordering of the initial signaling events of CD95. Mol. Cell. Biol. 22: 207–220
53. Kuwana T, Mackey MR, Perkins G, Ellisman MH, Latterich M, Schneiter R, Green DR and Newmeyer DD (2002) Bid, bax, and lipids cooperate to form supramolecular openings in the outer mitochondrial membrane. Cell 111: 331–342
54. Liu J, Chen J, Dai Q and Lee RM (2003) Phospholipid scramblase 3 is the mitochondrial target of protein kinase C γ-induced apoptosis. Cancer Res. 63: 1153–1156
55. Epand RF, Martinou JC, Montessuit S and Epand RM (2003) Transbilayer lipid diffusion promoted by Bax: implications for apoptosis. Biochemistry 42: 14576–14582
56. Hambrey PN and Mellors A (1975) Cardiolipin degradation by rat liver lysosomes. Biochem. Biophys. Res. Commun. 62: 939–945
57. Arur S, Uche UE, Rezaul K, Fong M, Scranton V, Cowan AE, Mohler W and Han DK (2003) Annexin I is an endogenous ligand that mediates apoptotic cell death engulfment. Dev. Cell 4: 587–598
58. Galve-de Rochemonteix B, Kobayashi T, Rosnoblet C, Lindsay M, Parton RG, Reber G, de Maistre E, Wahl D, Kruithof EK, Gruenberg J and de Moerloose P (2000) Interaction of anti-phospholipid antibodies with late endosomes of human endothelial cells. Arterioscler. Thromb. Vasc. Biol. 20: 563–574
59. Mc Neil HP, Krillis SA and Chesterman CN (1988) Purification of anti-phospholipid antibodies using a new affinity method. Thromb. Res. 52: 641–648
60. Tang DG, Chen YQ and Honn KV (1996) Arachidonate lipoxygenases as essential regulators of cell survival and apoptosis. Proc. Natl. Acad. Sci. USA 93: 5241–5246
61. Slee EA, Zhu H, Chow SC, MacFarlane M, Nicholson DW and Cohen GM (1996) Benzyloxycarbonyl-Val-Ala-Asp(O-Me) fluoromethyl ketone (z-VAD-FMK) inhibits apoptosis by blocking the processing CPP32. Biochem. J. 315: 21–24
62. Perdue JF (1974) The isolation and characterization of plasma membrane from cultured chicken embryo fibroblasts. Meth. Enzymol. 31: 162–168
63. Folch J, Lees M and Sloane-Stanley GH (1957) A simple method for the isolation and purification of total lipids from animal tissues. J. Biol. Chem. 226: 497–509
64. Fischer K, Chatterjee D, Torrelles J, Brennan PJ, Kaufmann SH and Schaible UE (2001) Mycobacterial lysocardiolipin is exported from phagosomes upon cleavage of cardiolipin by a macrophage-derived lysosomal phospholipase A2. J. Immunol. 167: 2187–2192
65. Hsu FF, Ma Z, Wohltmann M, Bohrer A, Nowatzke W, Ramanadham S and Turk J (2000) Electrospray ionization/mass spectrometric analyses of human promonocytic U937 cell glycerolipids and evidence that differentiation is associated with membrane lipid composition changes that facilitate phospholipase A2 activation. J. Biol. Chem. 275: 16579–16589
66. Petkovic M, Schiller J, Muller M, Bernard S, Reichl S, Arnold K and Arnhold J (2001) Detection of individual phospholipids in lipid mixtures by matrix-assisted laser desorption/ionization time-of-flight mass spectrometry. Anal. Biochem. 289: 202–216
67. Hancock K and Tsang VC (1983) India ink staining of proteins on nitrocellulose paper. Anal. Biochem. 133: 157–162